big data and cognitive computing

MDPI

Article

A Comparative Study for Stock Market Forecast Based on a New Machine Learning Model (Supplementary Material)

Enrique González-Núñez [1,*], Luis A. Trejo [1] and Michael Kampouridis [2]

[1] School of Engineering and Science, Tecnologico de Monterrey, Atizapán de Zaragoza 52926, Mexico; ltrejo@tec.mx
[2] School of Computer Science and Electronic Engineering, University of Essex, Wivenhoe Park, Colchester CO4 3SQ, Essex, UK; mkampo@essex.ac.uk
* Correspondence: enrique.gonzalez@tec.mx

S1. Results for the AHC models

This appendix contains complementary results for the experiments performed in Section 4.1, for the AHC models of the eight stock market indices.

Table S1. Statistical measures of the sum of squares and the R-square of the AHC model.

Training Model Performance				
Index	RSS	SSR	TSS	R-square
IPC	0.3444	144.0767	144.421	0.9976
S&P 500	0.5648	314.3745	314.9393	0.9982
DAX	0.5688	235.2522	235.8210	0.9976
DJIA	0.3454	276.9615	277.3069	0.9988
FTSE	0.3474	51.218	51.5654	0.9933
N225	0.6387	269.0818	269.7205	0.9976
NDX	0.8722	807.5651	808.4373	0.9989
CAC	0.4897	88.9595	89.4492	0.9945

Table S2. Descriptive statistics of the relative error.

Training Relative Error							
Index	Mean	Median	SD	MAD	Max	Min	Range
IPC	0.0008	0.0005	0.0009	0.0006	0.0104	0.0000	0.0104
S&P 500	0.0011	0.0006	0.0018	0.0009	0.0491	0.0000	0.0491
DAX	0.0011	0.0007	0.0014	0.0008	0.0388	0.0000	0.0388
DJIA	0.0008	0.0005	0.001	0.0006	0.0126	0.0000	0.0126
FTSE	0.0009	0.0006	0.0011	0.0007	0.0136	0.0000	0.0136
N225	0.0011	0.0007	0.0013	0.0008	0.0408	0.0000	0.0408
NDX	0.0012	0.0007	0.002	0.0009	0.0596	0.0000	0.0596
CAC	0.0011	0.0008	0.0013	0.0008	0.0247	0.0000	0.0247

Citation: González-Núñez, E.; Trejo, L. A.; Kampouridis, M. A Comparative Study for Stock Market Forecast Based on a New Machine Learning Model. *Big Data Cogn. Comput.* **2024**, *8*, 34. https://doi.org/10.3390/bdcc8040034

Academic Editor: Min Chen

Received: 25 January 2024
Revised: 3 March 2024
Accepted: 7 March 2024
Published: 26 March 2024

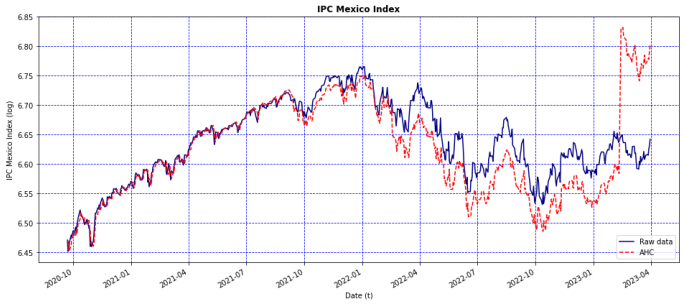

Figure S1. Graphs depicting the AHC model's forecast using the testing set of the S&P 500 (red line), and the original data (blue line).

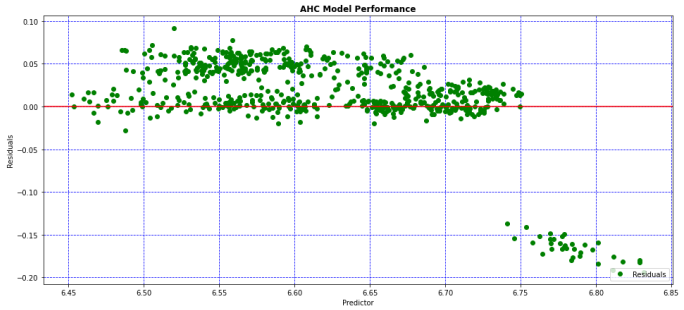

Figure S2. Residuals of the AHC model.

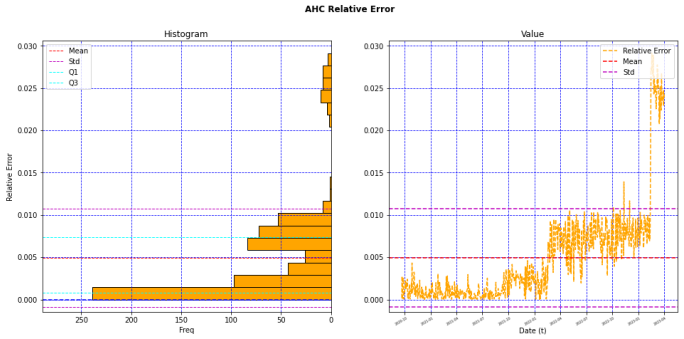

Figure S3. Behavior of the relative error of the AHC model.

Table S3. Structure of the computed AHC compound for the S&P 500 model: 12 molecules, and 16 coefficients per molecule.

Computed AHC model												
Molecule	1	2	3	4	5	6	7	8	9	10	11	12
τ	Cl	Cl	Cl	Cl	Ts	Cl	Cl	Ts	Ts	Ts	Cl	Ts
$\hat{a}_0$	0.4522	0.6039	0.5197	4.45×10^{-2}	4.4612	0.1731	9.54×10^{-2}	4.3854	4.1436	4.4865	2.2414	4.4277
$\hat{a}_1$	0.8939	0.9297	0.9482	0.8023	4.95×10^{-7}	0.9086	1.0131	1.48×10^{-6}	-9.38×10^{-6}	4.22×10^{-8}	0.8606	3.62×10^{-8}
$\hat{a}_2$	3.22×10^{-2}	1.64×10^{-3}	-7.54×10^{-2}	0.1913	4.84×10^{-7}	6.04×10^{-2}	-2.82×10^{-2}	1.72×10^{-6}	-1.02×10^{-5}	-4.33×10^{-8}	-0.1586	-4.61×10^{-8}
$\hat{a}_3$	-5.59×10^{-3}	9.46×10^{-2}	-0.14686	1.94×10^{-3}	5.56×10^{-5}	-6.45×10^{-3}	2.36×10^{-3}	3.52×10^{-5}	-8.19×10^{-4}	-8.58×10^{-7}	-0.1035	2.03×10^{-6}
$\hat{a}_4$	-2.27×10^{-3}	8.77×10^{-2}	-7.49×10^{-2}	4.40×10^{-3}	2.27×10^{-2}	1.95×10^{-3}	-3.23×10^{-4}	2.22×10^{-2}	2.63×10^{-2}	1.87×10^{-2}	-5.18×10^{-2}	2.09×10^{-2}
$\hat{a}_5$	-4.85×10^{-10}	-9.60×10^{-10}	-6.13×10^{-10}	8.29×10^{-10}	5.78×10^{-4}	4.86×10^{-10}	8.96×10^{-10}	2.90×10^{-3}	3.84×10^{-3}	-4.55×10^{-3}	-6.28×10^{-9}	1.89×10^{-3}
$\hat{a}_6$	-1.48×10^{-9}	-2.05×10^{-9}	-1.78×10^{-9}	6.53×10^{-11}	3.83×10^{-2}	-4.36×10^{-10}	-4.13×10^{-10}	3.47×10^{-3}	-5.75×10^{-3}	4.66×10^{-3}	-7.44×10^{-9}	9.70×10^{-2}
$\hat{a}_7$	-2.96×10^{-11}	-1.19×10^{-10}	2.30×10^{-12}	7.60×10^{-11}	1.01×10^{-8}	1.17×10^{-10}	6.96×10^{-12}	-7.74×10^{-11}	1.73×10^{-7}	1.03×10^{-9}	4.50×10^{-9}	3.75×10^{-9}
$\hat{a}_8$	-1.89×10^{-9}	-5.58×10^{-10}	-3.85×10^{-11}	8.81×10^{-12}	-4.96×10^{-6}	4.90×10^{-12}	-1.20×10^{-11}	-8.12×10^{-7}	1.51×10^{-5}	-2.64×10^{-8}	1.87×10^{-8}	2.70×10^{-7}
$\hat{a}_9$	-9.84×10^{-10}	-1.50×10^{-9}	-1.19×10^{-9}	4.44×10^{-10}	-4.99×10^{-6}	2.50×10^{-11}	2.41×10^{-10}	-9.36×10^{-7}	1.63×10^{-5}	1.35×10^{-8}	-6.86×10^{-9}	-4.68×10^{-9}
$\hat{a}_{10}$	-4.16×10^{-10}	-1.46×10^{-10}	4.31×10^{-11}	-3.36×10^{-11}	0	-3.98×10^{-11}	1.46×10^{-11}	0	0	0	-4.98×10^{-9}	0
$\hat{a}_{11}$	-6.80×10^{-10}	8.85×10^{-10}	2.66×10^{-10}	-2.77×10^{-11}	0	-8.98×10^{-12}	8.22×10^{-12}	0	0	0	-2.78×10^{-9}	0
$\hat{a}_{12}$	-6.18×10^{-10}	-1.95×10^{-10}	1.04×10^{-10}	-9.56×10^{-12}	0	-6.24×10^{-11}	-1.14×10^{-11}	0	0	0	-5.34×10^{-9}	0
$\hat{a}_{13}$	-2.30×10^{-5}	6.68×10^{-4}	-3.68×10^{-5}	-2.18×10^{-8}	0	1.92×10^{-6}	-1.15×10^{-9}	0	0	0	-2.71×10^{-3}	0
$\hat{a}_{14}$	-8.50×10^{-10}	1.42×10^{-10}	-4.17×10^{-11}	-5.16-13	0	4.58×10^{-11}	-1.26×10^{-11}	0	0	0	-1.52×10^{-8}	0
$\hat{a}_{15}$	0	0	0	0	0	0	0	0	0	0	0	0

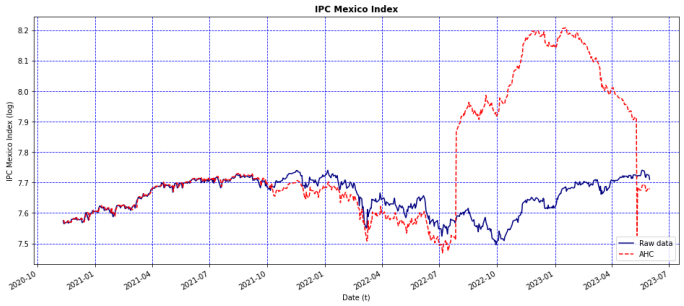

Figure S4. Graphs depicting the AHC model's forecast using the testing set of the DAX (red line), and the original data (blue line).

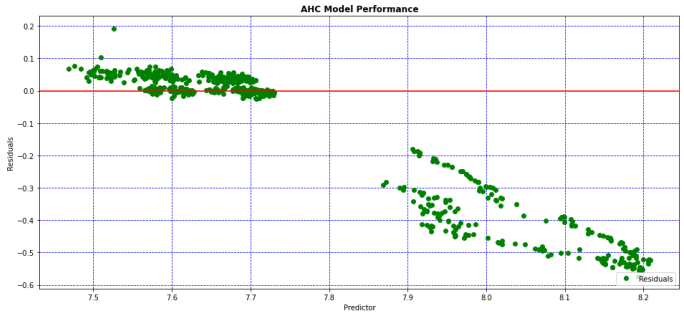

Figure S5. Residuals of the AHC model.

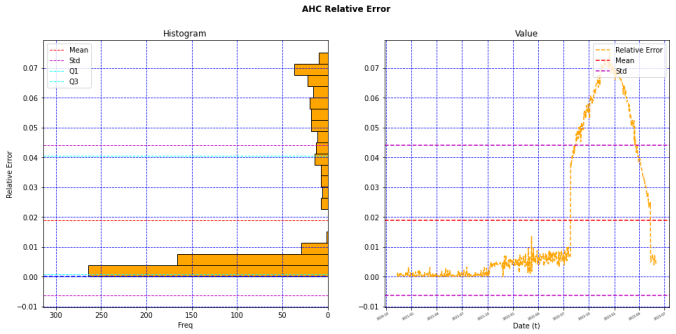

Figure S6. Behavior of the relative error of the AHC model.

Table S4. Structure of the computed AHC compound for the DAX model: 12 molecules, and 16 coefficients per molecule.

Computed AHC model												
Molecule	1	2	3	4	5	6	7	8	9	10	11	12
τ	Cl	Ts	Cl	Cl	Cl	Cl	Cl	Ts	Cl	Cl	Cl	Ts
$\hat{a}_0$	9.72×10^{-2}	5.5740	1.2376	0.7550	0.3083	0.5410	0.3908	6.0243	0.1496	0.3913	0.2199	6.0164
$\hat{a}_1$	0.9622	2.26×10^{-8}	0.7443	0.9350	0.9391	0.8836	0.9978	5.51×10^{-7}	0.9924	1.0178	0.8125	1.71×10^{-8}
$\hat{a}_2$	2.42×10^{-2}	1.91×10^{-8}	0.1031	-4.77×10^{-2}	2.45×10^{-2}	3.70×10^{-2}	-5.33×10^{-2}	5.68×10^{-7}	-1.26×10^{-2}	-7.06×10^{-2}	0.1029	1.83×10^{-8}
$\hat{a}_3$	3.14×10^{-3}	-2.73×10^{-5}	1.11×10^{-3}	4.28×10^{-3}	2.21×10^{-2}	1.67×10^{-2}	-5.01×10^{-4}	3.13×10^{-5}	3.57×10^{-3}	8.85×10^{-3}	-1.75×10^{-2}	-2.44×10^{-5}
$\hat{a}_4$	-2.87×10^{-3}	1.24×10^{-2}	4.47×10^{-2}	1.68×10^{-2}	6.28×10^{-3}	-4.84×10^{-2}	-1.40×10^{-2}	5.59×10^{-3}	-8.57×10^{-4}	4.18×10^{-3}	0.1032	7.91×10^{-3}
$\hat{a}_5$	8.83×10^{-10}	-1.36×10^{-3}	-5.66×10^{-9}	-2.40×10^{-9}	-1.44×10^{-10}	-1.37×10^{-9}	-5.26×10^{-10}	1.22×10^{-3}	6.46×10^{-10}	-6.70×10^{-10}	4.37×10^{-11}	2.63×10^{-4}
$\hat{a}_6$	-4.80×10^{-10}	-2.57×10^{-4}	-6.61×10^{-9}	-3.77×10^{-9}	-1.38×10^{-9}	-2.54×10^{-9}	-2.00×10^{-9}	0.7734	-8.45×10^{-10}	-2.29×10^{-9}	-9.60×10^{-10}	1.75×10^{-3}
$\hat{a}_7$	-1.84×10^{-11}	-4.66×10^{-10}	-1.79×10^{-9}	-1.89×10^{-9}	-3.47×10^{-10}	-1.25×10^{-10}	9.74×10^{-10}	3.27×10^{-9}	9.40×10^{-12}	-6.17×10^{-11}	-2.99×10^{-11}	-1.63×10^{-10}
$\hat{a}_8$	-1.21×10^{-11}	-3.82×10^{-8}	-6.30×10^{-10}	-5.86×10^{-10}	8.05×10^{-11}	-9.78×10^{-12}	1.86×10^{-11}	2.72×10^{-7}	-6.01×10^{-11}	-1.88×10^{-10}	-1.35×10^{-10}	-8.22×10^{-8}
$\hat{a}_9$	2.01×10^{-10}	-3.32×10^{-8}	-6.14×10^{-9}	-3.08×10^{-9}	-7.65×10^{-10}	-1.95×10^{-9}	-1.26×10^{-9}	2.72×10^{-7}	-9.86×10^{-11}	-1.48×10^{-9}	4.57×10^{-10}	-6.88×10^{-8}
$\hat{a}_{10}$	-1.37×10^{-11}	0	-6.35×10^{-10}	1.00×10^{-9}	4.34×10^{-10}	5.79×10^{-10}	1.33×10^{-10}	0	6.00×10^{-12}	-2.90×10^{-10}	2.24×10^{-10}	0
$\hat{a}_{11}$	-3.37×10^{-11}	0	2.11×10^{-9}	-1.23×10^{-9}	-1.82×10^{-10}	-1.85×10^{-10}	-2.46×10^{-11}	0	3.14×10^{-11}	4.38×10^{-10}	-1.56×10^{-10}	0
$\hat{a}_{12}$	5.54×10^{-11}	0	-7.23×10^{-10}	1.28×10^{-9}	7.43×10^{-10}	7.48×10^{-10}	1.59×10^{-10}	0	8.09×10^{-12}	-4.52×10^{-10}	4.27×10^{-10}	0
$\hat{a}_{13}$	-6.39×10^{-8}	0	8.34×10^{-5}	8.27×10^{-5}	1.38×10^{-6}	-1.06×10^{-7}	-3.37×10^{-7}	0	4.22×10^{-6}	2.19×10^{-5}	-1.57×10^{-4}	0
$\hat{a}_{14}$	-2.09×10^{-11}	0	-1.18×10^{-10}	1.18×10^{-10}	3.69×10^{-10}	3.70×10^{-11}	-1.96×10^{-10}	0	1.67×10^{-11}	1.37×10^{-10}	2.19×10^{-10}	0
$\hat{a}_{15}$	0	0	0	0	0	0	0	0	0	0	0	0

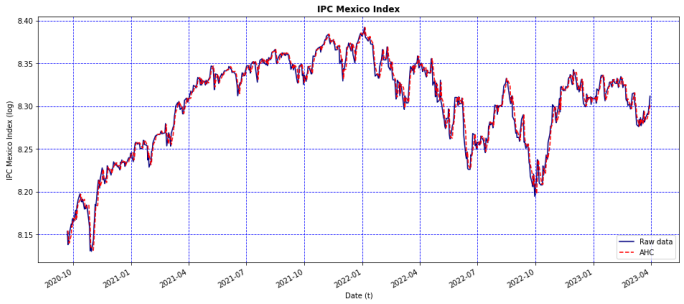

Figure S7. Graphs depicting the AHC model's forecast using the testing set of the DJIA (red line), and the original data (blue line).

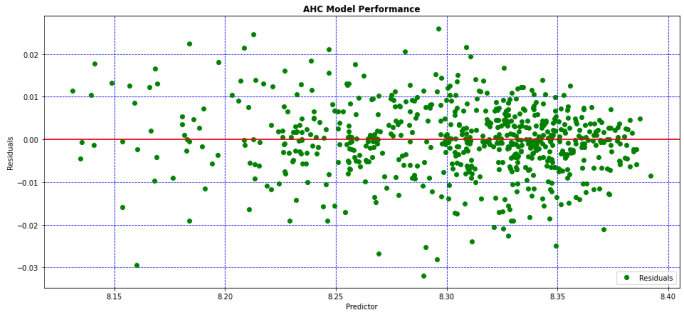

Figure S8. Residuals of the AHC model.

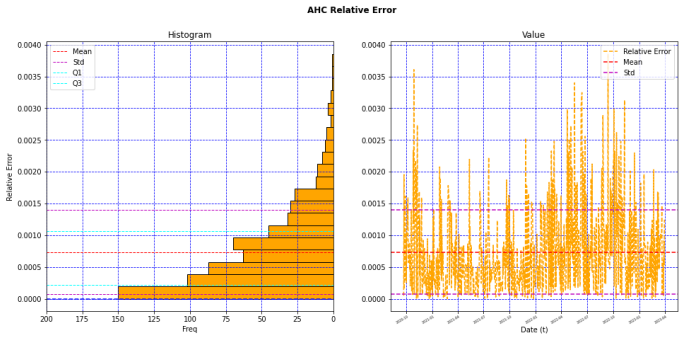

Figure S9. Behavior of the relative error of the AHC model.

Table S5. Structure of the computed AHC compound for the DJIA model: two molecules, and 16 coefficients per molecule.

Computed AHC model		
Molecule	1	2
τ	Cl	Cl
$\hat{a}_0$	9.40×10^{-3}	6.77×10^{-2}
$\hat{a}_1$	0.8449	0.8601
$\hat{a}_2$	0.1538	0.1311
$\hat{a}_3$	-2.42×10^{-4}	-3.83×10^{-3}
$\hat{a}_4$	7.84×10^{-5}	3.79×10^{-3}
$\hat{a}_5$	1.26×10^{-9}	8.96×10^{-10}
$\hat{a}_6$	1.79×10^{-10}	-1.66×10^{-10}
$\hat{a}_7$	-1.02×10^{-10}	-2.63×10^{-11}
$\hat{a}_8$	1.58×10^{-10}	6.18×10^{-11}
$\hat{a}_9$	7.21×10^{-10}	3.64×10^{-10}
$\hat{a}_{10}$	3.43×10^{-12}	3.82×10^{-11}
$\hat{a}_{11}$	-3.54×10^{-11}	4.82×10^{-14}
$\hat{a}_{12}$	9.52×10^{-12}	-2.45×10^{-11}
$\hat{a}_{13}$	-2.20×10^{-8}	-2.80×10^{-8}
$\hat{a}_{14}$	-1.78×10^{-10}	3.45×10^{-11}
$\hat{a}_{15}$	0	0

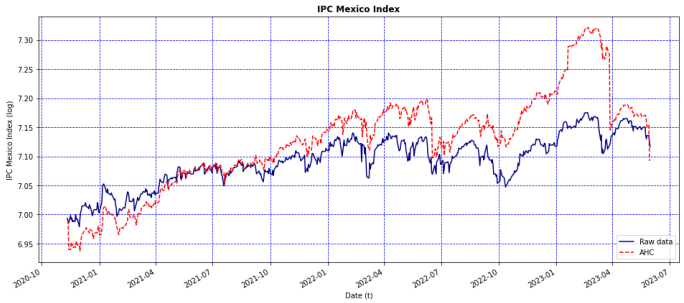

Figure S10. Graphs depicting the AHC model's forecast using the testing set of the FTSE (red line), and the original data (blue line).

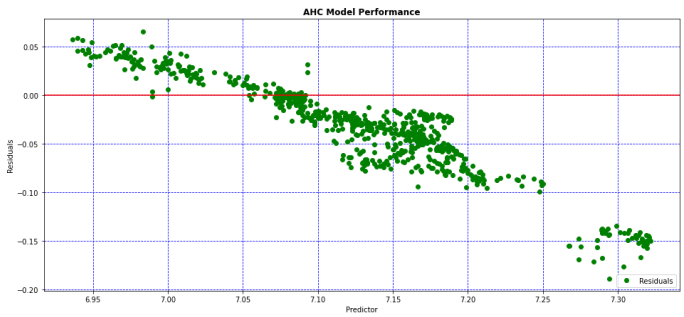

Figure S11. Residuals of the AHC model.

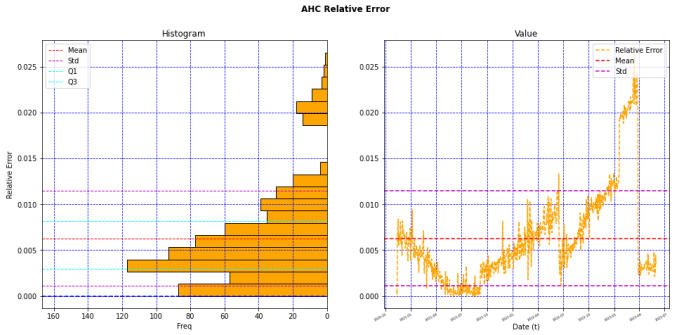

Figure S12. Behavior of the relative error of the AHC model.

Table S6. Structure of the computed AHC compound for the FTSE model: 12 molecules, and 16 coefficients per molecule.

Computed AHC model												
Molecule	1	2	3	4	5	6	7	8	9	10	11	12
τ	Cl	Cl	Cl	Cl	Cl	Cl	Cl	Cl	Cl	Ts	Ts	Ts
$\hat{a}_0$	0.4846	0.6342	0.1676	0.6157	0.4328	0.5910	0.6893	0.2214	0.8477	5.6342	5.4929	5.5194
$\hat{a}_1$	0.9109	0.9175	0.9739	1.0274	1.0005	0.8924	0.9610	0.8933	0.8187	-9.08×10^{-10}	8.84×10^{-10}	6.76×10^{-10}
$\hat{a}_2$	9.60×10^{-3}	1.73×10^{-2}	1.68×10^{-3}	-0.1235	-5.45×10^{-2}	2.47×10^{-2}	-9.21×10^{-2}	7.86×10^{-2}	4.64×10^{-2}	1.16×10^{-8}	3.32×10^{-8}	-1.01×10^{-7}
$\hat{a}_3$	6.73×10^{-2}	-2.48×10^{-2}	2.17×10^{-3}	6.00×10^{-2}	1.80×10^{-2}	1.29×10^{-3}	0.1325	1.13×10^{-2}	-0.1025	-4.86×10^{-6}	-1.79×10^{-5}	-3.75×10^{-6}
$\hat{a}_4$	2.48×10^{-2}	0.1079	4.11×10^{-3}	3.04×10^{-2}	2.79×10^{-2}	5.55×10^{-3}	-0.4471	1.16×10^{-2}	5.14×10^{-2}	8.35×10^{-3}	1.18×10^{-2}	1.30×10^{-2}
$\hat{a}_5$	-9.50×10^{-10}	-1.82×10^{-9}	5.37×10^{-10}	-1.56×10^{-9}	-7.10×10^{-10}	-1.67×10^{-9}	-1.96×10^{-9}	1.51×10^{-10}	-2.99×10^{-9}	1.55×10^{-3}	-1.84×10^{-5}	-1.45×10^{-3}
$\hat{a}_6$	2.15×10^{-9}	-3.08×10^{-9}	-8.14×10^{-10}	-3.16×10^{-9}	-2.18×10^{-9}	2.89×10^{-9}	3.41×10^{-9}	-1.00×10^{-9}	-4.06×10^{-9}	6.03×10^{-2}	-1.04×10^{-3}	-1.99×10^{-3}
$\hat{a}_7$	-6.77×10^{-11}	-2.07×10^{-9}	-6.71×10^{-11}	-1.33×10^{-10}	9.80×10^{-11}	1.46×10^{-10}	-5.15×10^{-10}	-1.38×10^{-10}	-1.47×10^{-10}	8.56×10^{-11}	8.55×10^{-11}	3.75×10^{-10}
$\hat{a}_8$	1.12×10^{-11}	-2.15×10^{-10}	3.93×10^{-11}	-7.53×10^{-10}	9.17×10^{-11}	2.47×10^{-10}	-7.70×10^{-12}	-8.88×10^{-11}	-1.07×10^{-9}	-1.10×10^{-8}	-2.88×10^{-9}	-5.08×10^{-9}
$\hat{a}_9$	-1.55×10^{-9}	-2.45×10^{-9}	-1.38×10^{-10}	-2.36×10^{-9}	-1.44×10^{-9}	-2.28×10^{-9}	2.68×10^{-9}	-4.28×10^{-10}	-3.53×10^{-9}	-2.24×10^{-8}	-2.89×10^{-8}	3.90×10^{-8}
$\hat{a}_{10}$	-7.38×10^{-11}	-3.27×10^{-10}	4.13×10^{-11}	-4.30×10^{-10}	1.32×10^{-10}	4.25×10^{-11}	-9.43×10^{-10}	1.25×10^{-10}	-5.13×10^{-10}	0	0	0
$\hat{a}_{11}$	-6.76×10^{-11}	5.77×10^{-10}	1.31×10^{-11}	-1.33×10^{-9}	3.67×10^{-10}	5.13×10^{-10}	1.30×10^{-10}	2.17×10^{-11}	-1.77×10^{-9}	0	0	0
$\hat{a}_{12}$	1.11×10^{-10}	-4.46×10^{-10}	2.39×10^{-10}	5.80×10^{-10}	2.01×10^{-10}	9.12×10^{-11}	1.16×10^{-9}	2.69×10^{-10}	-5.90×10^{-10}	0	0	0
$\hat{a}_{13}$	1.12×10^{-6}	3.13×10^{-4}	2.51×10^{-8}	5.57×10^{-4}	2.61×10^{-5}	7.04×10^{-6}	-5.50×10^{-4}	5.87×10^{-7}	1.45×10^{-4}	0	0	0
$\hat{a}_{14}$	9.70×10^{-11}	-2.35×10^{-10}	-2.33×10^{-11}	-2.84×10^{-10}	2.61×10^{-5}	-3.73×10^{-10}	1.39×10^{-10}	6.72×10^{-11}	-3.78×10^{-10}	0	0	0
$\hat{a}_{15}$	0	0	0	0	0	0	0	0	0	0	0	0

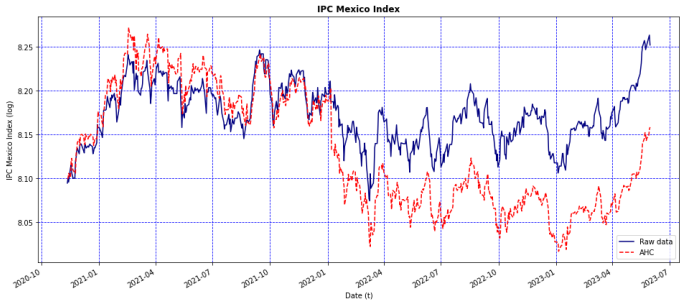

Figure S13. Graphs depicting the AHC model's forecast using the testing set of the N225 (red line), and the original data (blue line).

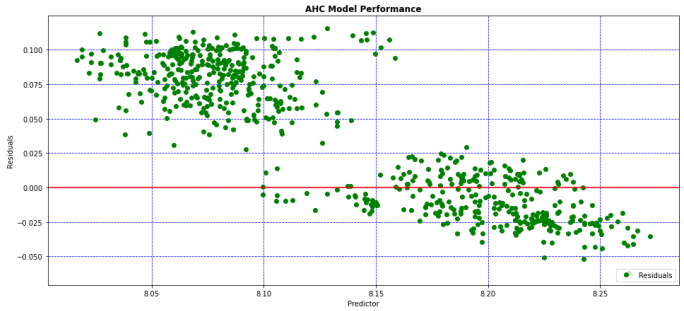

Figure S14. Residuals of the AHC model.

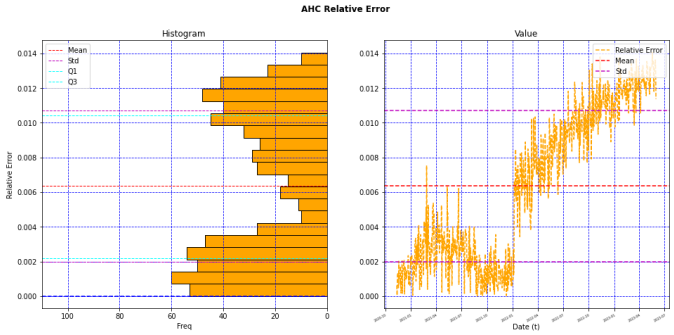

Figure S15. Behavior of the relative error of the AHC model.

Table S7. Structure of the computed AHC compound for the N225 model: 12 molecules, and 16 coefficients per molecule.

Computed AHC model												
Molecule	1	2	3	4	5	6	7	8	9	10	11	12
τ	Cl	Cl	Cl	Cl	Cl	Cl	Ts	Cl	Cl	Cl	Cl	Ts
$\hat{a}_0$	0.1397	1.4097	0.1689	0.4703	0.2436	0.4436	6.2383	0.6471	1.1404	0.1798	0.6008	5.9325
$\hat{a}_1$	0.9190	0.9242	0.9020	0.9719	0.9729	0.8707	-2.51×10^{-9}	0.8778	0.9375	0.7989	0.9517	-2.07×10^{-7}
$\hat{a}_2$	6.33×10^{-2}	-9.64×10^{-2}	7.63×10^{-2}	-3.07×10^{-2}	-5.78×10^{-3}	4.47×10^{-2}	-6.46×10^{-9}	3.63×10^{-2}	8.00×10^{-2}	0.1506	-2.28×10^{-2}	-2.20×10^{-7}
$\hat{a}_3$	-1.22×10^{-3}	0.2383	7.02×10^{-4}	-1.11×10^{-2}	3.67×10^{-3}	-7.77×10^{-2}	-6.18×10^{-8}	-8.41×10^{-3}	0.1776	5.37×10^{-2}	4.09×10^{-2}	3.12×10^{-6}
$\hat{a}_4$	7.66×10^{-4}	-2.86×10^{-2}	-4.03×10^{-4}	-3.45×10^{-3}	1.53×10^{-3}	3.63×10^{-2}	7.07×10^{-3}	9.45×10^{-3}	-6.47×10^{-2}	-2.58×10^{-2}	-1.65×10^{-2}	8.68×10^{-3}
$\hat{a}_5$	5.81×10^{-10}	-6.22×10^{-9}	3.74×10^{-10}	-1.39×10^{-9}	1.22×10^{-10}	-1.03×10^{-9}	-2.79×10^{-4}	-2.54×10^{-9}	-5.28×10^{-9}	2.03×10^{-10}	-1.85×10^{-9}	-2.03×10^{-4}
$\hat{a}_6$	-7.67×10^{-10}	-7.72×10^{-9}	-9.09×10^{-10}	-2.95×10^{-9}	-1.30×10^{-9}	-2.22×10^{-9}	1.54×10^{-2}	-3.84×10^{-9}	-6.84×10^{-9}	-7.70×10^{-10}	-3.29×10^{-9}	8.58×10^{-3}
$\hat{a}_7$	2.62×10^{-10}	-2.49×10^{-11}	4.93×10^{-10}	-3.00×10^{-10}	5.35×10^{-11}	7.94×10^{-11}	5.05×10^{-11}	-5.03×10^{-10}	-2.97×10^{-10}	2.14×10^{-11}	1.88×10^{-10}	3.19×10^{-9}
$\hat{a}_8$	3.84×10^{-10}	3.87×10^{-9}	2.44×10^{-10}	-1.93×10^{-9}	-1.34×10^{-10}	-1.90×10^{-9}	2.21×10^{-10}	6.01×10^{-10}	-8.30×10^{-10}	-3.63×10^{-10}	2.65×10^{-10}	7.29×10^{-8}
$\hat{a}_9$	-9.41×10^{-11}	-6.97×10^{-9}	-2.67×10^{-10}	-2.18×10^{-9}	-5.89×10^{-10}	-1.62×10^{-9}	1.73×10^{-9}	-3.19×10^{-9}	6.06×10^{-9}	-2.83×10^{-10}	-2.57×10^{-9}	3.35×10^{-8}
$\hat{a}_{10}$	2.81×10^{-12}	4.09×10^{-10}	1.60×10^{-11}	1.05×10^{-10}	-1.42×10^{-11}	-3.84×10^{-10}	0	7.66×10^{-10}	-1.31×10^{-9}	-9.05×10^{-12}	-9.62×10^{-11}	0
$\hat{a}_{11}$	-1.57×10^{-11}	-2.85×10^{-9}	4.34×10^{-11}	-3.81×10^{-10}	3.50×10^{-10}	-1.72×10^{-9}	0	-1.73×10^{-10}	2.61×10^{-9}	2.67×10^{-10}	-1.96×10^{-9}	0
$\hat{a}_{12}$	7.79×10^{-11}	4.41×10^{-10}	8.85×10^{-11}	1.22×10^{-10}	5.34×10^{-13}	-4.77×10^{-10}	0	9.01×10^{-10}	-1.47×10^{-9}	9.92×10^{-11}	-1.27×10^{-10}	0
$\hat{a}_{13}$	5.29×10^{-8}	-1.77×10^{-4}	-3.75×10^{-8}	-1.04×10^{-6}	2.08×10^{-6}	-4.86×10^{-5}	0	4.71×10^{-6}	-3.44×10^{-4}	7.12×10^{-5}	-3.28×10^{-4}	0
$\hat{a}_{14}$	1.97×10^{-10}	5.05×10^{-10}	-1.68×10^{-10}	-9.98×10^{-10}	-2.73×10^{-11}	-1.97×10^{-10}	0	3.57×10^{-10}	5.47×10^{-10}	1.27×10^{-10}	5.48×10^{-10}	0
$\hat{a}_{15}$	0	0	0	0	0	0	0	0	0	0	0	0

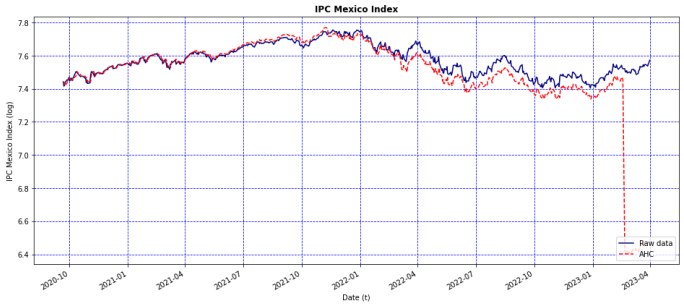

Figure S16. Graphs depicting the AHC model's forecast using the testing set of the NDX (red line), and the original data (blue line).

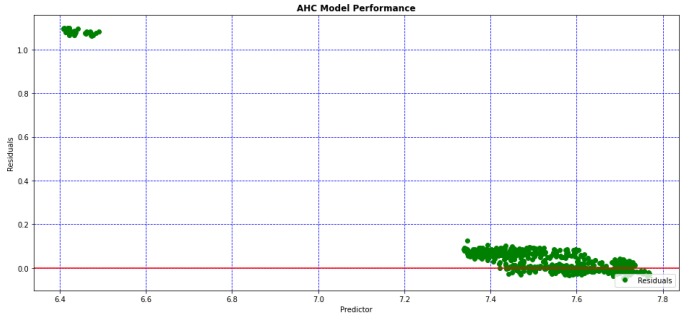

Figure S17. Residuals of the AHC model.

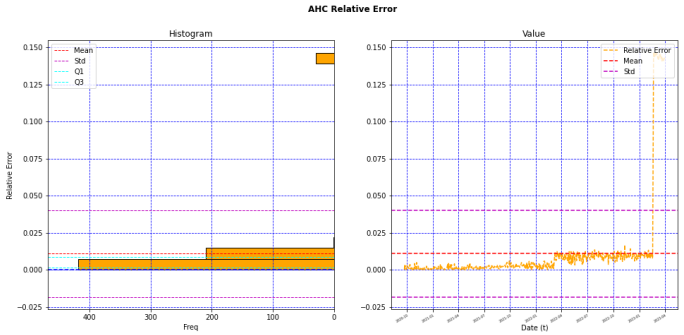

Figure S18. Behavior of the relative error of the AHC model.

Table S8. Structure of the computed AHC compound for the NDX model: 12 molecules, and 16 coefficients per molecule.

Computed AHC model												
Molecule	1	2	3	4	5	6	7	8	9	10	11	12
τ	Cl	Ts	Cl	Ts	Cl	Cl	Cl	Cl	Ts	Cl	Cl	Ts
$\hat{a}_0$	2.25×10^{-2}	4.7814	0.4064	5.0013	0.2237	9.69×10^{-2}	0.4639	-9.12×10^{-2}	4.5989	0.5763	2.4683	4.9469
$\hat{a}_1$	0.8319	7.68×10^{-7}	0.9439	3.17×10^{-7}	0.9339	0.9750	0.9597	0.7347	-3.46×10^{-7}	0.9793	0.9480	-1.16×10^{-7}
$\hat{a}_2$	0.1660	1.11×10^{-6}	-7.40×10^{-3}	3.01×10^{-7}	2.21×10^{-2}	1.11×10^{-2}	-3.25×10^{-2}	0.2490	2.37×10^{-7}	-3.07×10^{-2}	-0.1593	-9.90×10^{-8}
$\hat{a}_3$	2.99×10^{-3}	-9.72×10^{-4}	-6.02×10^{-3}	-8.71×10^{-6}	5.12×10^{-3}	3.72×10^{-3}	1.45×10^{-2}	0.1284	-3.92×10^{-5}	9.59×10^{-2}	-0.2286	6.30×10^{-5}
$\hat{a}_4$	8.50×10^{-3}	2.03×10^{-2}	-2.67×10^{-3}	1.59×10^{-2}	-4.35×10^{-2}	-2.34×10^{-4}	3.08×10^{-3}	-4.54×10^{-2}	1.95×10^{-2}	0.1043	-0.1253	1.59×10^{-2}
$\hat{a}_5$	1.05×10^{-9}	-7.34×10^{-4}	-3.25×10^{-10}	-1.14×10^{-4}	3.46×10^{-10}	8.91×10^{-10}	-5.85×10^{-10}	1.19×10^{-9}	1.37×10^{-3}	-1.00×10^{-9}	-7.32×10^{-9}	3.01×10^{-4}
$\hat{a}_6$	1.22×10^{-10}	-5.17×10^{-2}	-1.46×10^{-9}	4.55×10^{-2}	-7.13×10^{-10}	-4.62×10^{-10}	-1.81×10^{-9}	6.16×10^{-10}	1.59×10^{-2}	-2.28×10^{-9}	-8.61×10^{-9}	6.64×10^{-2}
$\hat{a}_7$	5.76×10^{-11}	1.48×10^{-7}	4.72×10^{-11}	-4.80×10^{-10}	2.21×10^{-10}	1.28×10^{-11}	-2.31×10^{-12}	3.49×10^{-11}	-6.89×10^{-10}	-1.45×10^{-10}	8.81×10^{-9}	-3.08×10^{-8}
$\hat{a}_8$	-2.32×10^{-12}	1.12×10^{-5}	-2.01×10^{-9}	-9.01×10^{-7}	2.67×10^{-11}	-1.61×10^{-11}	-1.85×10^{-11}	-1.14×10^{-10}	1.74×10^{-7}	-6.01×10^{-10}	4.13×10^{-8}	-6.07×10^{-6}
$\hat{a}_9$	5.82×10^{-10}	1.29×10^{-5}	-8.94×10^{-10}	-9.06×10^{-7}	-1.83×10^{-10}	2.14×10^{-10}	-1.19×10^{-9}	9.04×10^{-10}	-1.08×10^{-7}	-1.64×10^{-9}	-7.97×10^{-9}	-6.01×10^{-6}
$\hat{a}_{10}$	-4.66×10^{-11}	0	-3.84×10^{-10}	0	-6.89×10^{-11}	1.52×10^{-11}	1.25×10^{-10}	2.61×10^{-10}	0	-9.81×10^{-11}	-4.69×10^{-9}	0
$\hat{a}_{11}$	-3.12×10^{-11}	0	-5.34×10^{-10}	0	-2.17×10^{-11}	7.29×10^{-12}	3.04×10^{-10}	-8.12×10^{-12}	0	8.98×10^{-10}	-5.07×10^{-9}	0
$\hat{a}_{12}$	-2.92×10^{-11}	0	-6.16×10^{-10}	0	-9.21×10^{-11}	-9.08×10^{-12}	1.84×10^{-10}	1.89×10^{-10}	0	-1.56×10^{-10}	-5.01×10^{-9}	0
$\hat{a}_{13}$	-2.20×10^{-8}	0	-9.07×10^{-6}	0	1.61×10^{-6}	-3.54×10^{-9}	-1.46×10^{-6}	1.78×10^{-7}	0	1.13×10^{-3}	-3.85×10^{-3}	0
$\hat{a}_{14}$	7.30×10^{-12}	0	-9.13×10^{-10}	0	8.77×10^{-11}	-1.06×10^{-11}	-8.84×10^{-11}	-5.22×10^{-11}	0	1.78×10^{-10}	-2.61×10^{-8}	0
$\hat{a}_{15}$	0	0	0	0	0	0	0	0	0	0	0	0

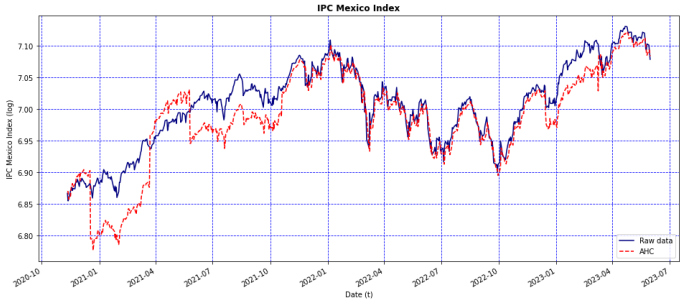

Figure S19. Graphs depicting the AHC model's forecast using the testing set of the CAC (red line), and the original data (blue line).

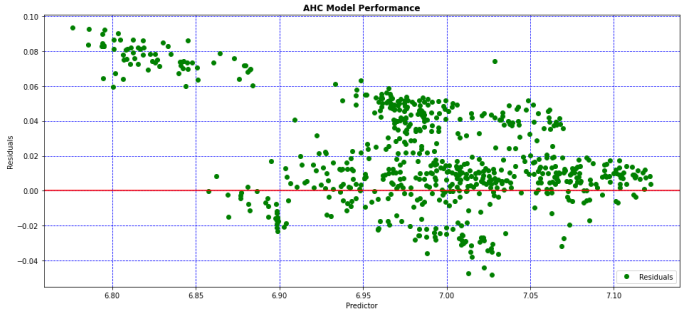

Figure S20. Residuals of the AHC model.

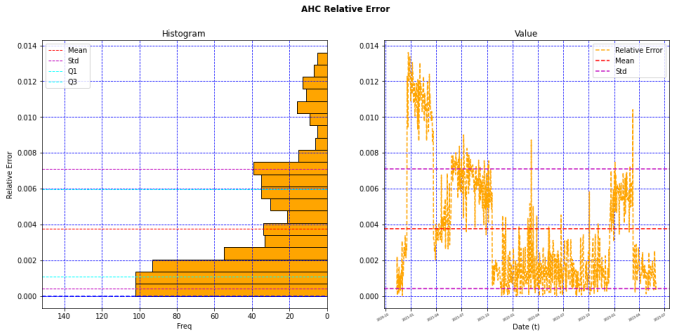

Figure S21. Behavior of the relative error of the AHC model.

Table S9. Structure of the computed AHC compound for the CAC model: 12 molecules, and 16 coefficients per molecule.

Computed AHC model												
Molecule	1	2	3	4	5	6	7	8	9	10	11	12
τ	Cl	Cl	Cl	Cl	Ts	Cl	Ts	Cl	Ts	Cl	Ts	Ts
$\hat{a}_0$	0.6775	0.5439	0.1171	0.5087	5.4072	0.2000	5.0702	4.24×10^{-2}	5.2244	1.0449	5.4264	5.5299
$\hat{a}_1$	1.0262	0.9265	0.9239	1.0264	1.25×10^{-8}	0.9376	-2.14×10^{-8}	0.9422	3.20×10^{-7}	0.8424	-5.02×10^{-7}	1.16×10^{-8}
$\hat{a}_2$	-0.1271	-5.69×10^{-3}	5.26×10^{-2}	-8.59×10^{-2}	3.67×10^{-8}	2.86×10^{-2}	-3.42×10^{-8}	3.09×10^{-2}	3.27×10^{-7}	2.65×10^{-2}	-1.62×10^{-7}	1.48×10^{-8}
$\hat{a}_3$	-1.67×10^{-2}	-1.37×10^{-3}	1.34×10^{-2}	4.40×10^{-2}	2.27×10^{-5}	6.61×10^{-3}	-1.17×10^{-4}	-6.98×10^{-2}	-2.02×10^{-4}	2.72×10^{-2}	4.87×10^{-5}	2.39×10^{-7}
$\hat{a}_4$	-3.63×10^{-3}	9.80×10^{-3}	1.10×10^{-2}	-1.31×10^{-2}	1.29×10^{-2}	-2.93×10^{-3}	1.64×10^{-2}	-2.64×10^{-2}	1.21×10^{-2}	-3.88×10^{-2}	9.82×10^{-3}	1.38×10^{-2}
$\hat{a}_5$	-1.72×10^{-9}	-1.16×10^{-9}	7.18×10^{-10}	-9.82×10^{-10}	-2.93×10^{-4}	3.75×10^{-10}	-6.33×10^{-4}	1.07×10^{-9}	2.24×10^{-3}	-3.76×10^{-9}	2.49×10^{-3}	1.75×10^{-3}
$\hat{a}_6$	-3.29×10^{-9}	-2.40×10^{-9}	-4.78×10^{-10}	-2.50×10^{-9}	-2.63×10^{-2}	-7.99×10^{-10}	-3.62×10^{-3}	-1.48×10^{-10}	-4.01×10^{-3}	-4.88×10^{-9}	-2.24×10^{-4}	-0.2577
$\hat{a}_7$	-5.04×10^{-10}	2.81×10^{-10}	-8.51×10^{-11}	-1.18×10^{-10}	-6.09×10^{-10}	-1.21×10^{-10}	1.58×10^{-9}	7.66×10^{-12}	3.63×10^{-9}	1.36×10^{-11}	5.37×10^{-10}	6.41×10^{-10}
$\hat{a}_8$	2.48×10^{-9}	1.90×10^{-10}	-1.23×10^{-11}	3.81×10^{-10}	1.35×10^{-8}	1.10×10^{-10}	2.30×10^{-7}	-2.52×10^{-11}	-1.96×10^{-7}	-7.73×10^{-10}	2.47×10^{-7}	1.59×10^{-8}
$\hat{a}_9$	-2.50×10^{-9}	-1.78×10^{-9}	1.20×10^{-10}	-1.74×10^{-9}	1.56×10^{-8}	-2.12×10^{-10}	1.16×10^{-7}	4.63×10^{-10}	-1.97×10^{-7}	-4.32×10^{-9}	7.57×10^{-8}	2.05×10^{-8}
$\hat{a}_{10}$	2.93×10^{-10}	1.73×10^{-10}	2.98×10^{-11}	4.16×10^{-10}	0	-1.04×10^{-10}	0	-1.09×10^{-10}	0	8.19×10^{-10}	0	0
$\hat{a}_{11}$	-7.02×10^{-10}	5.98×10^{-10}	3.34×10^{-11}	-5.99×10^{-10}	0	1.14×10^{-11}	0	-1.94×10^{-10}	0	-1.83×10^{-9}	0	0
$\hat{a}_{12}$	3.73×10^{-10}	2.58×10^{-10}	-1.63×10^{-10}	5.93×10^{-10}	0	-3.43×10^{-10}	0	-2.01×10^{-11}	0	9.23×10^{-10}	0	0
$\hat{a}_{13}$	-2.35×10^{-6}	5.02×10^{-6}	-5.65×10^{-7}	-2.73×10^{-5}	0	-4.26×10^{-8}	0	1.75×10^{-6}	0	-1.37×10^{-3}	0	0
$\hat{a}_{14}$	1.14×10^{-9}	-1.37×10^{-10}	-7.19×10^{-12}	3.38×10^{-10}	0	1.50×10^{-10}	0	1.45×10^{-11}	0	5.29×10^{-10}	0	0
$\hat{a}_{15}$	0	0	0	0	0	0	0	0	0	0	0	0

S2. Results for the GA models

This appendix contains complementary results for the experiments performed in Section 4.2, for the GA models of the eight stock market indices.

Table S10. Statistical measures of the sum of squares and the R-square of the GA model.

Training Model Performance				
Index	RSS	SSR	TSS	R-square
IPC	42.2446	194.8260	237.0707	0.8218
S&P 500	641.9862	1279.5598	1921.5461	0.6659
DAX	156.7972	479.4217	636.2190	0.7535
DJIA	51.4930	436.5324	488.0255	0.8944
FTSE	647.7246	649.5375	1297.2621	0.5006
N225	428.2488	890.9307	1319.1796	0.6753
NDX	243.5902	741.9016	985.4919	0.7528
CAC	533.4923	451.6153	985.1077	0.4584

Table S11. Descriptive statistics of the relative error.

Training Relative Error							
Index	Mean	Median	SD	MAD	Max	Min	Range
IPC	0.0104	0.0092	0.0069	0.0060	0.0310	0.0000	0.0310
S&P 500	0.0536	0.0425	0.0452	0.0385	0.1712	0.0000	0.1712
DAX	0.0226	0.0186	0.0172	0.0133	0.1707	0.0000	0.1707
DJIA	0.0115	0.0091	0.0101	0.0078	0.1047	0.0000	0.1047
FTSE	0.0560	0.0571	0.0191	0.0151	0.0997	0.0000	0.0997
N225	0.0386	0.0388	0.0226	0.0189	0.1197	0.0000	0.1197
NDX	0.0335	0.0328	0.0227	0.0191	0.1177	0.0000	0.1177
CAC	0.0459	0.0430	0.0310	0.0256	0.1888	0.0000	0.1888

Table S12. Computed GA's genotype with the coefficients (Genes) for the S&P 500 model.

Computed GA model	
Gene	Value
$\hat{a}_0$	-11.705950
$\hat{a}_1$	0.138040
$\hat{a}_2$	2.813108
$\hat{a}_3$	0.133460
$\hat{a}_4$	0.121590
$\hat{a}_5$	-8.937811
$\hat{a}_6$	-10.742956
$\hat{a}_7$	-11.568881
$\hat{a}_8$	9.965202
$\hat{a}_9$	-11.894175
$\hat{a}_{10}$	-11.298640
$\hat{a}_{11}$	8.690697
$\hat{a}_{12}$	-11.116551
$\hat{a}_{13}$	10.605489
$\hat{a}_{14}$	-9.878893

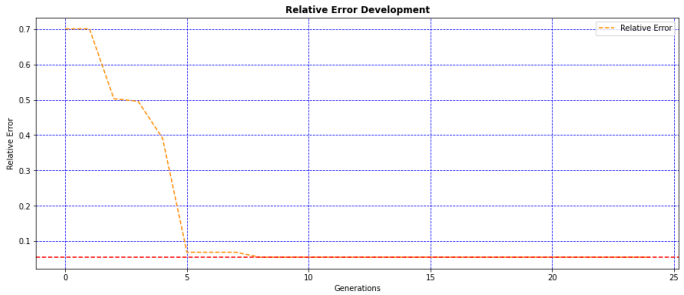

Figure S22. S&P 500 error behavior through 25 generations.

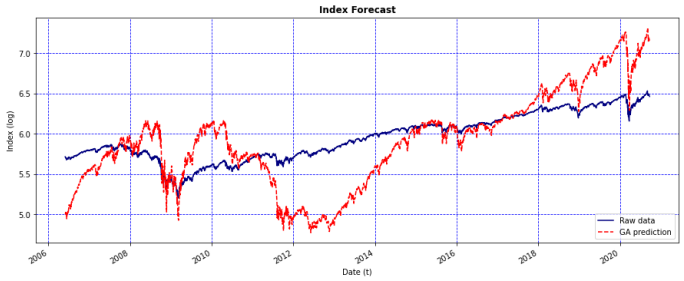

Figure S23. Curves for the S&P 500 training forecast (red line), and the original data (blue line).

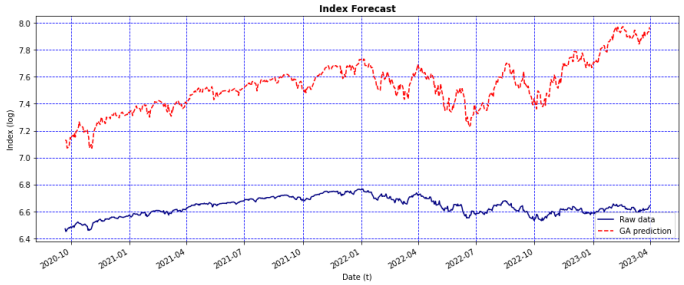

Figure S24. Graphs depicting the GA model's forecast using the testing set of the S&P 500 (red line), and the original data (blue line).

Table S13. Computed GA's genotype with the coefficients (Genes) for the DAX model.

Computed GA model	
Gene	Value
$\hat{a}_0$	4.351814
$\hat{a}_1$	-9.228633
$\hat{a}_2$	9.625772
$\hat{a}_3$	4.459086×10^{-3}
$\hat{a}_4$	-0.131584
$\hat{a}_5$	-10.252599
$\hat{a}_6$	-11.415722
$\hat{a}_7$	8.936730
$\hat{a}_8$	-1.445764
$\hat{a}_9$	-11.593349
$\hat{a}_{10}$	5.158250
$\hat{a}_{11}$	10.604330
$\hat{a}_{12}$	9.924640
$\hat{a}_{13}$	10.591934
$\hat{a}_{14}$	6.926830

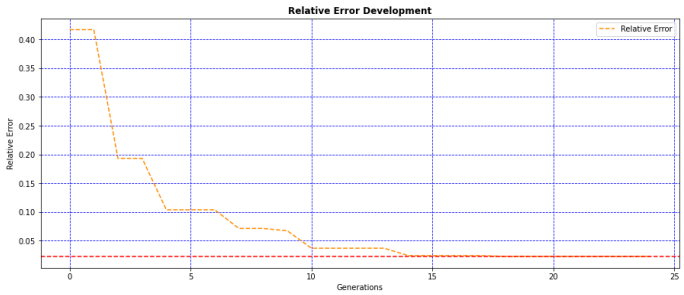

Figure S25. DAX error behavior through 25 generations.

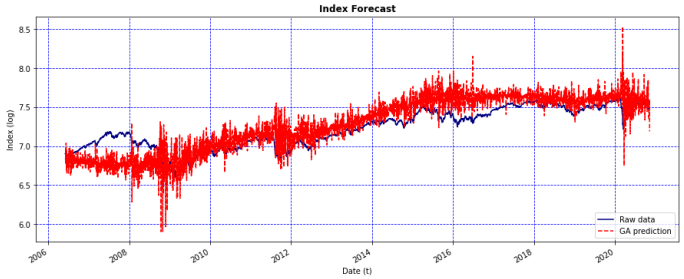

Figure S26. Curves for the DAX training forecast (red line), and the original data (blue line).

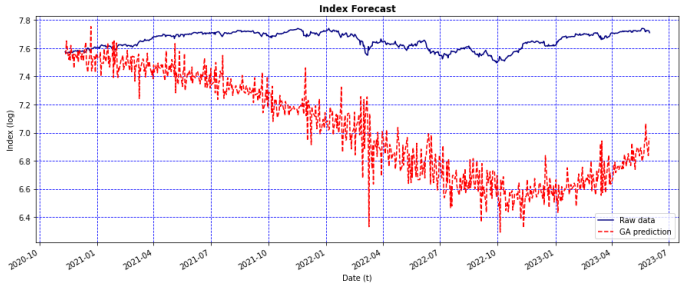

Figure S27. Graphs depicting the GA model's forecast using the testing set of the DAX (red line), and the original data (blue line).

Computed GA model	
Gene	Value
$\hat{a}_0$	-2.690749
$\hat{a}_1$	-6.064102
$\hat{a}_2$	7.410093
$\hat{a}_3$	1.717362×10^{-2}
$\hat{a}_4$	-2.617421×10^{-2}
$\hat{a}_5$	8.634908
$\hat{a}_6$	11.453117
$\hat{a}_7$	5.881121
$\hat{a}_8$	5.954249
$\hat{a}_9$	10.514256
$\hat{a}_{10}$	-7.029368
$\hat{a}_{11}$	4.977630
$\hat{a}_{12}$	-6.085035
$\hat{a}_{13}$	10.456973
$\hat{a}_{14}$	-11.483238

Table S14. Computed GA's genotype with the coefficients (Genes) for the DJIA model.

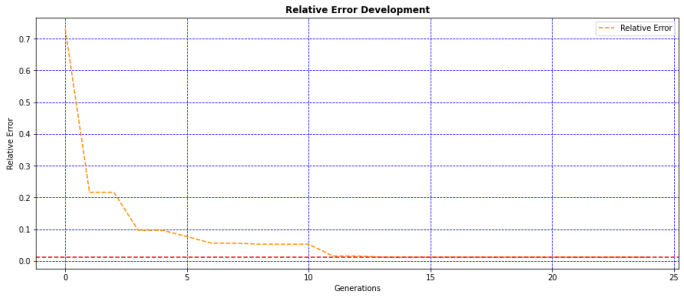

Figure S28. DJIA error behavior through 25 generations.

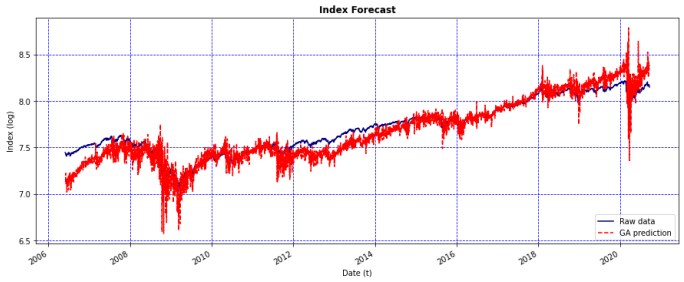

Figure S29. Curves for the DJIA training forecast (red line), and the original data (blue line).

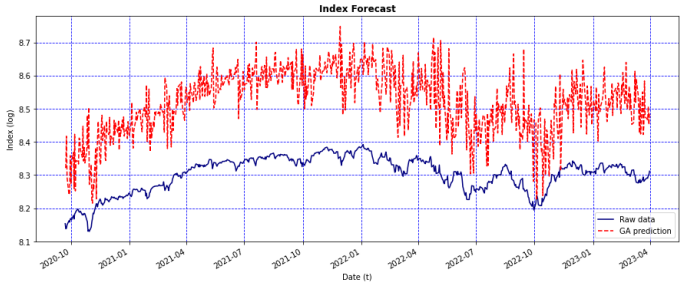

Figure S30. Graphs depicting the GA model's forecast using the testing set of the DJIA (red line), and the original data (blue line).

Computed GA model	
Gene	Value
$\hat{a}_0$	11.537824
$\hat{a}_1$	2.087738
$\hat{a}_2$	-2.794673
$\hat{a}_3$	-3.570098×10^{-2}
$\hat{a}_4$	-7.697125×10^{-2}
$\hat{a}_5$	7.835915
$\hat{a}_6$	11.481279
$\hat{a}_7$	4.830762
$\hat{a}_8$	11.247838
$\hat{a}_9$	9.018821
$\hat{a}_{10}$	11.701948
$\hat{a}_{11}$	9.038480
$\hat{a}_{12}$	10.244514
$\hat{a}_{13}$	9.299599
$\hat{a}_{14}$	-4.390437

Table S15. Computed GA's genotype with the coefficients (Genes) for the FTSE model.

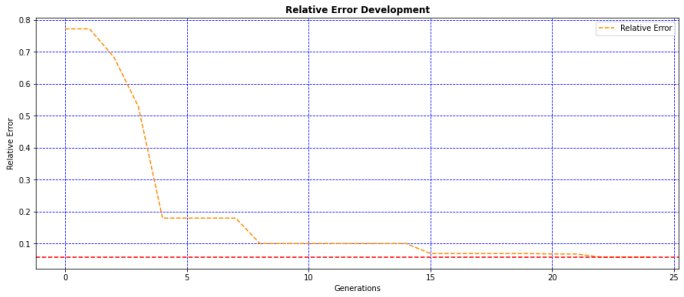

Figure S31. FTSE error behavior through 25 generations.

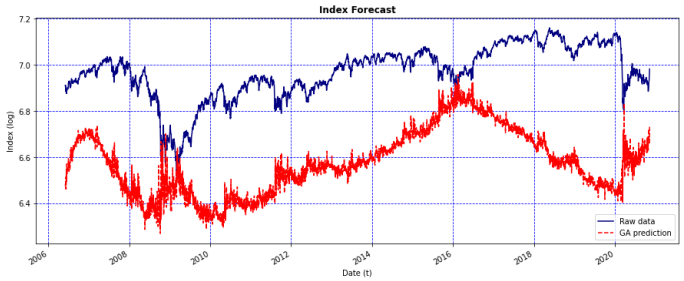

Figure S32. Curves for the FTSE training forecast (red line), and the original data (blue line).

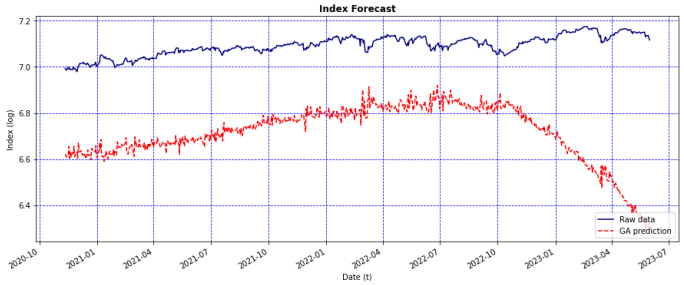

Figure S33. Graphs depicting the GA model's forecast using the testing set of the FTSE (red line), and the original data (blue line).

Computed GA model	
Gene	Value
$\hat{a}_0$	2.825819
$\hat{a}_1$	-4.166251
$\hat{a}_2$	4.763972
$\hat{a}_3$	1.298465×10^{-2}
$\hat{a}_4$	-0.136210
$\hat{a}_5$	3.931826
$\hat{a}_6$	-10.222616
$\hat{a}_7$	-3.352121
$\hat{a}_8$	0.620355
$\hat{a}_9$	-10.920465
$\hat{a}_{10}$	7.231079
$\hat{a}_{11}$	6.218989
$\hat{a}_{12}$	4.678560
$\hat{a}_{13}$	5.344712
$\hat{a}_{14}$	2.355904

Table S16. Computed GA's genotype with the coefficients (Genes) for the N225 model.

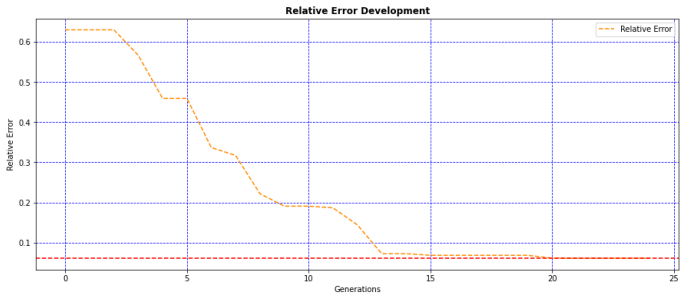

Figure S34. N225 error behavior through 25 generations.

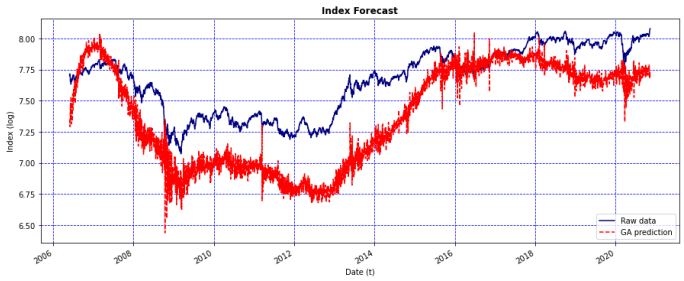

Figure S35. Curves for the N225 training forecast (red line), and the original data (blue line).

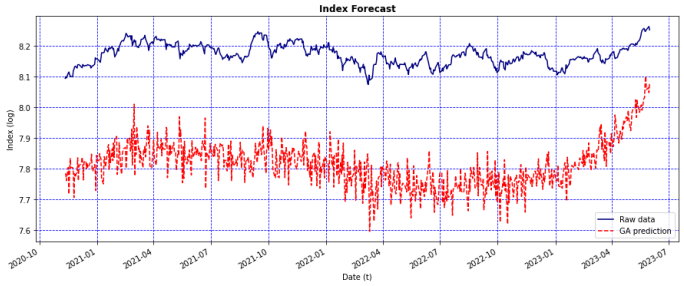

Figure S36. Graphs depicting the GA model's forecast using the testing set of the N225 (red line), and the original data (blue line).

Computed GA model	
Gene	Value
$\hat{a}_0$	-2.815794
$\hat{a}_1$	5.126774
$\hat{a}_2$	-3.718289
$\hat{a}_3$	7.577315×10^{-2}
$\hat{a}_4$	0.175781
$\hat{a}_5$	9.471851
$\hat{a}_6$	10.666745
$\hat{a}_7$	-10.546244
$\hat{a}_8$	-5.262695
$\hat{a}_9$	10.520163
$\hat{a}_{10}$	-11.312181
$\hat{a}_{11}$	6.860403
$\hat{a}_{12}$	-11.348953
$\hat{a}_{13}$	-8.072384
$\hat{a}_{14}$	-9.382521

Table S17. Computed GA's genotype with the coefficients (Genes) for the NDX model.

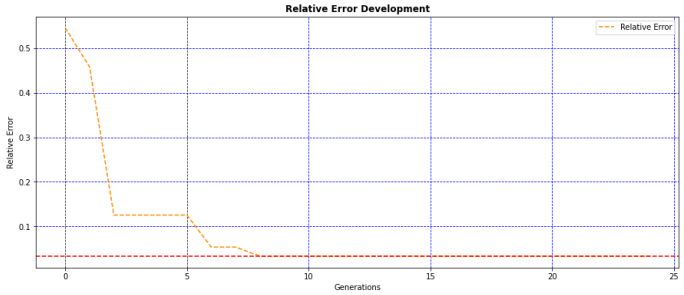

Figure S37. NDX error behavior through 25 generations.

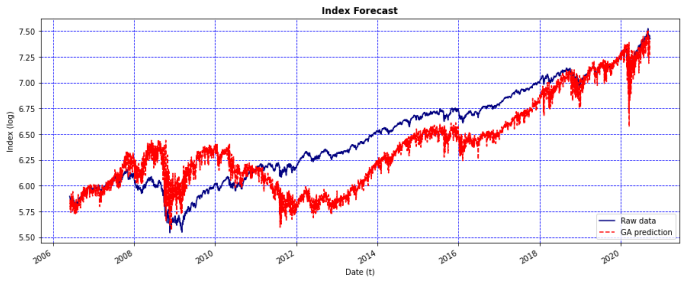

Figure S38. Curves for the NDX training forecast (red line), and the original data (blue line).

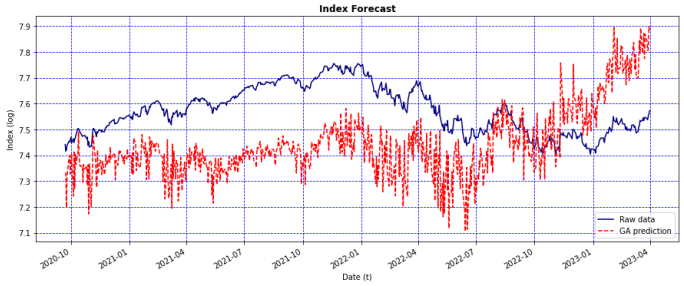

Figure S39. Graphs depicting the GA model's forecast using the testing set of the NDX (red line), and the original data (blue line).

Computed GA model	
Gene	Value
$\hat{a}_0$	3.055734
$\hat{a}_1$	-9.676661
$\hat{a}_2$	10.192865
$\hat{a}_3$	-3.125075×10^{-2}
$\hat{a}_4$	0.121814
$\hat{a}_5$	11.299048
$\hat{a}_6$	11.557959
$\hat{a}_7$	11.347721
$\hat{a}_8$	-10.336681
$\hat{a}_9$	11.272740
$\hat{a}_{10}$	5.092625
$\hat{a}_{11}$	-8.637655
$\hat{a}_{12}$	10.066735
$\hat{a}_{13}$	-8.942899
$\hat{a}_{14}$	-7.666530

Table S18. Computed GA's genotype with the coefficients (Genes) for the CAC model.

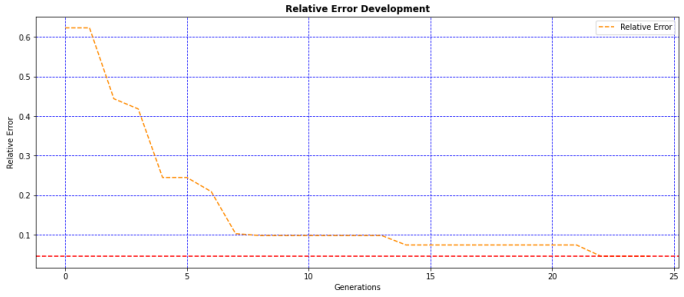

Figure S40. CAC error behavior through 25 generations.

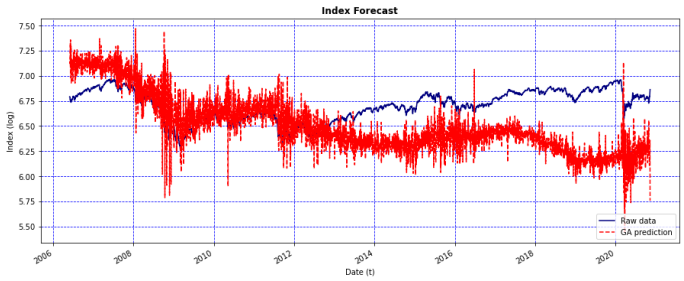

Figure S41. Curves for the CAC training forecast (red line), and the original data (blue line).

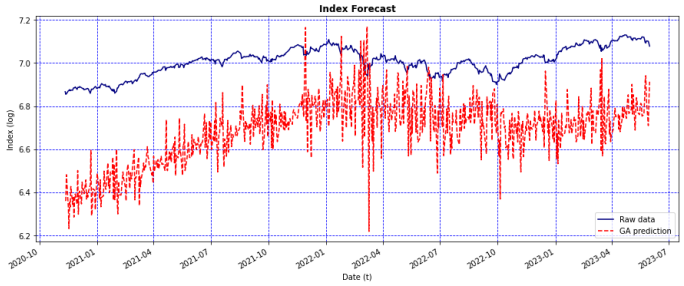

Figure S42. Graphs depicting the GA model's forecast using the testing set of the CAC (red line), and the original data (blue line).

S3. Results for the Buy-and-Hold Strategy

This appendix contains complementary results for the experiments performed in Section 4.4, for the implementation of the Buy-and-Hold strategy of the rest of the indices.

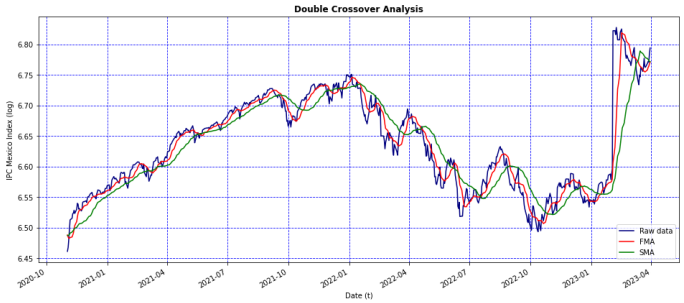

Figure S43. Curves of the S&P 500 forecast (blue line), with the 10-day FMA (red line), and 30-day SMA frames (green line).

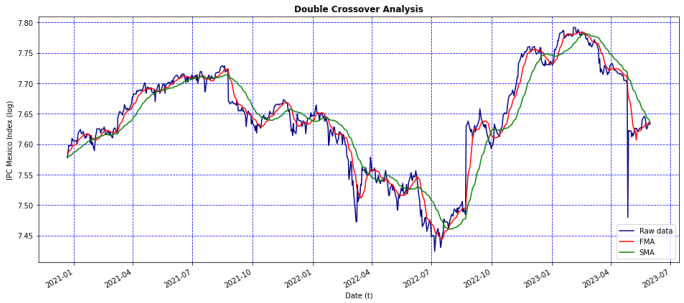

Figure S44. Curves of the DAX forecast (blue line), with the 10-day FMA (red line), and 30-day SMA frames (green line).

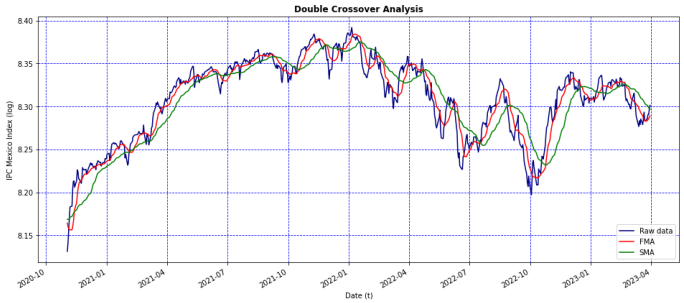

Figure S45. Curves of the DJIA forecast (blue line), with the 10-day FMA (red line), and 30-day SMA frames (green line).

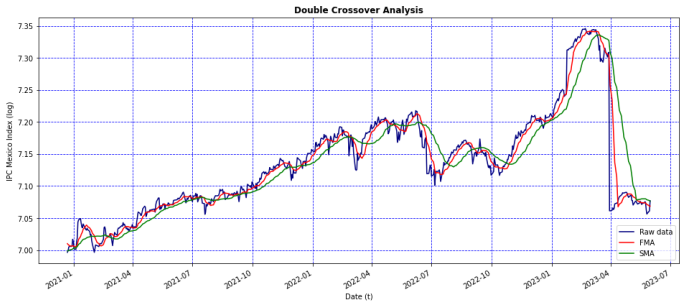

Figure S46. Curves of the FTSE forecast (blue line), with the 10-day FMA (red line), and 30-day SMA frames (green line).

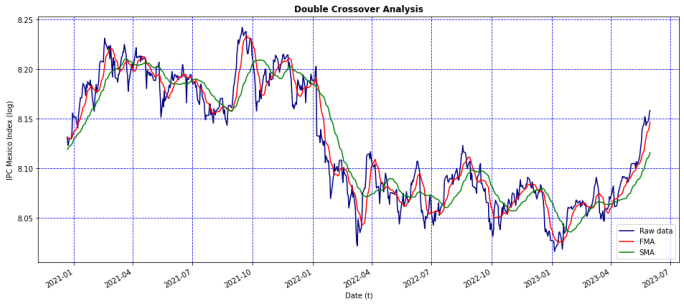

Figure S47. Curves of the N225 forecast (blue line), with the 10-day FMA (red line), and 30-day SMA frames (green line).

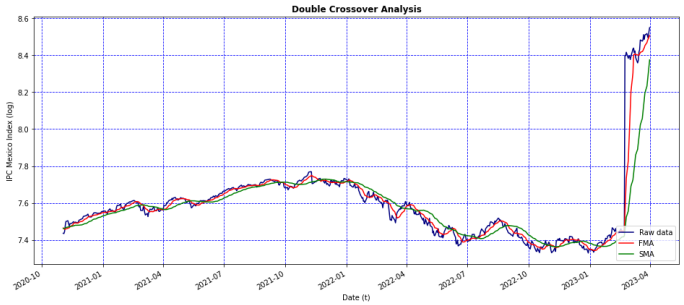

Figure S48. Curves of the NDX forecast (blue line), with the 10-day FMA (red line), and 30-day SMA frames (green line).

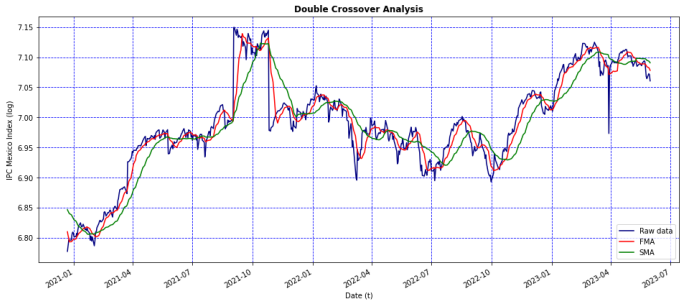

Figure S49. Curves of the CAC forecast (blue line), with the 10-day FMA (red line), and 30-day SMA frames (green line).